Y.-G. Jung, I.M. Peterson, D.K. Kim, and B.R. Lawn*

Materials Science and Engineering Laboratory, Building 223, Room B309, National Institute of Standards and Technology, Gaithersburg, Maryland 20899, USA; *corresponding author, brian.lawn@nist.gov

Lifetime-limiting Strength Degradation from Contact Fatigue in Dental Ceramics

ABSTRACT

The hypothesis under examination in this paper is that the lifetimes of dental restorations are limited by the accumulation of contact damage during oral function; and, moreover, that strengths of dental ceramics are significantly lower after multi-cycle loading than after single-cycle loading. Accordingly, indentation damage and associated strength degradation from multi-cycle contacts with spherical indenters in water are evaluated in four dental ceramics: "aesthetic" ceramics—porcelain and micaceous glass-ceramic (MGC), and "structural" ceramics—glass-infiltrated alumina and yttria-stabilized tetragonal zirconia polycrystal (Y-TZP). At large numbers of contact cycles, all materials show an abrupt transition in damage mode, consisting of strongly enhanced damage inside the contact area and attendant initiation of radial cracks outside. This transition in damage mode is not observed in comparative static loading tests, attesting to a strong mechanical component in the fatigue mechanism. Radial cracks, once formed, lead to rapid degradation in strength properties, signaling the end of the useful lifetime of the material. Strength degradation from multi-cycle contacts is examined in the test materials, after indentation at loads from 200 to 3000 N up to 10^6 cycles. Degradation occurs in the porcelain and MGC after $\approx 10^4$ cycles at loads as low as 200 N; comparable degradation in the alumina and Y-TZP requires loads higher than 500 N, well above the clinically significant range.

KEY WORDS: contact fatigue, damage accumulation, dental ceramics, fracture, strength degradation.

INTRODUCTION

All-ceramic crowns are superior to traditional porcelain-fused-to-metal crowns in aesthetics, wear resistance, and chemical inertness (Giordano, 1996). Quantitative data on clinical performance have not been extensively documented, but some existing studies (Hankinson and Cappetta, 1994; Kelly et al., 1995; Kelsey et al., 1995; Kelly, 1997) indicate a tendency for all-ceramic crowns to fail after a few years in the mouth—i.e., "fatigue" failure. Molar crowns are subject to a demanding environment—typical histories involve > 10^7 biting cycles at loads up to and even above 200 N over contacts between opposing cusps of characteristic radii 2 to 4 mm, in aqueous solutions (Wheeler, 1958; DeLong and Douglas, 1983; Anusavice, 1989; Phillips, 1991; Craig, 1997; Kelly, 1997). It is well-known that ceramics are susceptible to progressive "slow" growth of cracks in tension, particularly in the presence of environmental water (Wiederhorn, 1967). Traditionally, the influence of slow crack growth on strength is evaluated by means of "dynamic fatigue" tests, in which the strength of bend specimens is measured as a function of crosshead speed in a mechanical loading machine (Ritter, 1978). Cyclic loading enhances this susceptibility (Ritchie, 1988; Lathabai and Lawn, 1989; Lathabai et al., 1989, 1991; Dauskardt et al., 1990; Suresh, 1991). The influence of slow crack growth from pre-existent surface flaws as a tensile failure mechanism in dental ceramics has been demonstrated in cyclic flexure tests on a feldspathic porcelain (Fairhurst et al., 1993).

However, it is only recently that fatigue responses of structural ceramics in loading with spherical contacts more closely representative of the predominantly compressive contact conditions in oral function have been documented (Guiberteau et al., 1993; Cai et al., 1994b; Pajares et al., 1995b; Lee and Lawn, 1999). Fundamentally different damage modes are observed in contact loading, depending on the ceramic microstructure: In homogeneous, fine-grain microstructures, conical cracks form at the specimen surface around the contact circle ("Hertzian cone" fractures), where limited tension occurs ("brittle" mode) (Hertz, 1896; Frank and Lawn, 1967; Lawn and Wilshaw, 1975; Lawn, 1993); in heterogeneous, coarse-grain microstructures, distributed microcracks develop within a subsurface zone below the contact, driven by shear stresses ("quasi-plastic" mode) (Lawn et al., 1994). The latter kind of damage has been studied in our laboratories in single-cycle loading in a broad range of dental ceramics (Peterson et al., 1998a). Some work on the strength degradation properties of dental ceramics from multi-cycle contacts has begun to appear in the literature (White et al., 1995, 1997; Peterson et al., 1998b; Jung et al., 1999a); however, underlying mechanisms of cyclic failure, particularly from quasi-plasticity, have not been explicitly identified or quantified.

In this paper, we investigate the cyclic contact fatigue properties of several dental ceramics using "blunt" spherical indenters (Lawn and Wilshaw, 1975; Lawn, 1993), in water. The selected ceramics are the same as or are similar to those used in our preceding study of single-cycle damage (Peterson et al., 1998a): aesthetic ceramics, a feldspathic porcelain, and a micaceous

glass-ceramic, in use as overlaying veneers and inlays or onlays; and structural ceramics, a glass-infiltrated alumina and an yttria-stabilized tetragonal polycrystal zirconia, in use and under development as underlying cores in crowns. We show that the same cone-crack and *quasi*-plastic damage modes operate as in single-cycle loading, but that more deleterious crack systems develop at large numbers of cycles, leading to accelerated failure. These additional crack systems include "radial" cracks associated with advanced *quasi*-plasticity, analogous to the radial cracks produced in "sharp" contacts (*e.g.*, Vickers or Knoop diamond pyramid indenters) (Lawn and Wilshaw, 1975; Lawn, 1993). The radial cracks are not observed in comparative static loading, indicating a strong mechanical (in addition to chemical) component in the cyclic damage. And even under severe cyclic loading conditions where they do occur, they may not be easy to detect by conventional observation techniques. It is hypothesized that advanced cyclic damage accumulation limits the potential long-lifetime performance of dental ceramics: specifically, that strength after multi-cycle contact damage is significantly lower than after single-cycle damage. We argue that Hertzian contact tests more closely simulate oral function than more traditional tests, such as dynamic fatigue, and may thereby provide deeper insights into relevant modes of failure in dental ceramics. Lifetime characteristics are quantified by measuring the strengths of flexure test specimens after contact testing.

MATERIALS & METHODS

Materials Preparation and Characterization

As indicated above, porcelain, micaceous glass-ceramic, and glass-infiltrated alumina dental ceramics from an earlier study (Peterson *et al.*, 1998a) are used here. The basic microstructures of these materials are described in an earlier paper (Peterson *et al.*, 1998a). One material, a finer-grain zirconia, is substituted for an otherwise similar material in that earlier paper. These are all essentially dense materials (< 1% porosity).

Feldspathic Porcelain

(Vita Mark II®, Vita Zahnfabrik, Bad Säckingen, Germany). The microstructure consists of a glass matrix and reinforcing sanidine crystalline phase particles of size 3 to 7 μm with some undissolved frit of size 1 to 7 μm.

Micaceous Glass-Ceramic

(MGC, Corning Inc., Corning, NY). The mica has the form of blocky platelets, volume fraction ≈ 0.60, with platelet thickness ≈ 0.7 μm and diameter ≈ 3 μm, in a glassy bonding phase.

Glass-infiltrated Alumina

(Vita Celay In-Ceram, Vita Zahnfabrik, Bad Säckingen, Germany). The initially porous dry-pressed alumina pre-form is infiltrated with ≈ 0.30 volume fraction lanthanum-aluminosilicate glass, resulting in an alumina superstructure with bonding glass.

Yttria-stabilized Tetragonal Zirconia Polycrystal

(Y-TZP, Norton-St. Gobain, Raleigh, NC, USA). The material is a polycrystalline zirconia containing 3 mol% yttria-stabilizing additive, with an equi-axed microstructure of mean grain size ≈ 0.5 μm, and with insignificant grain boundary phase. (This

compares with a grain size ≈ 1 μm for the Y-TZP used in our previous study.)

Bar specimens 3 x 4 x 25 mm were cut from blocks of each material and polished to finer than 1 μm diamond paste for contact testing and subsequent strength testing.

Contact Fatigue Testing

Indentation tests were carried out with tungsten carbide spheres of radius r = 3.18 mm as previously described (Peterson *et al.*, 1998a), but with additional provision for repeat loading over n cycles at prescribed load P (Guiberteau *et al.*, 1993; Cai *et al.*, 1994b; Pajares *et al.*, 1995b; Peterson *et al.*, 1998b; Lee and Lawn, 1999). Our procedure uses hard tungsten carbide spheres to minimize fatigue of the indenters themselves—a radius 3.18 mm is selected in the midrange of cuspal radii (2 to 4 mm). The indenter is mounted on the underside of the crosshead on a hydraulic testing machine (Instron Model 8502, Instron Corp., Canton, MA, USA), and the specimen is centrally aligned along the load axis. The specimen is raised until light contact is made with the sphere, and the load is then applied. The ensuing contact area has an inverse relation to the stiffness of the material.

Cyclic tests were carried out at a frequency f = 10 Hz, in haversinusoidal wave form. The load was cycled between a specified maximum (typically 200 N, but up to 3000 N) and small but non-zero minimum (< 20 N, to avoid lateral translation of the sphere during the test). Some static tests over a prescribed hold time at maximum load P = 500 N were conducted for comparative purposes. All tests were performed with the contact area immersed in distilled water. A minimum of five specimens was indented at each given load and number of cycles.

Damage sites were observed in reflection optical microscopy by Nomarski interference contrast (Peterson *et al.*, 1998a). Selected porcelain, MGC, and alumina specimens were sectioned from the back surface to a final thickness ≈ 0.5 mm with a 10-μm-grit diamond wheel followed by 1-μm diamond paste. The thinned, translucent specimens were then viewed in transmission optical microscopy, which highlighted any subsurface cracks. The latter observational procedure was not useful for the Y-TZP, owing to the relatively high opacity of this material.

Indented specimens were then placed in a four-point bend fixture (inner span, 10 mm; outer span, 20 mm) with the damage site centrally located on the tensile side. So that rate effects from the incursion of moisture in this stage of testing would be minimized, the indentation sites were dried and covered with a drop of silicone oil; the specimens were then broken in fast fracture (time to fracture < 40 ms), yielding "inert strengths" (Marshall and Lawn, 1980).

We examined all broken surfaces by optical microscopy to observe the contact damage and to determine fracture origins (Peterson *et al.*, 1998a). Of those specimens that failed from indentation sites, a select few were gold-coated for photography in Nomarski interference contrast.

One-way ANOVA was used to quantify the significance of strength data trends.

RESULTS

The effect of multi-cycle contact loading on strength is demonstrated in Figs. 1-5 for porcelain, MGC, glass-infiltrated alumina, and Y-TZP. In all materials, the strengths
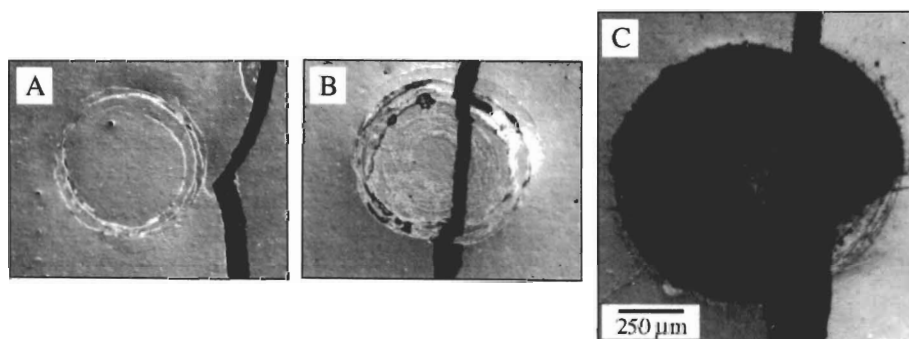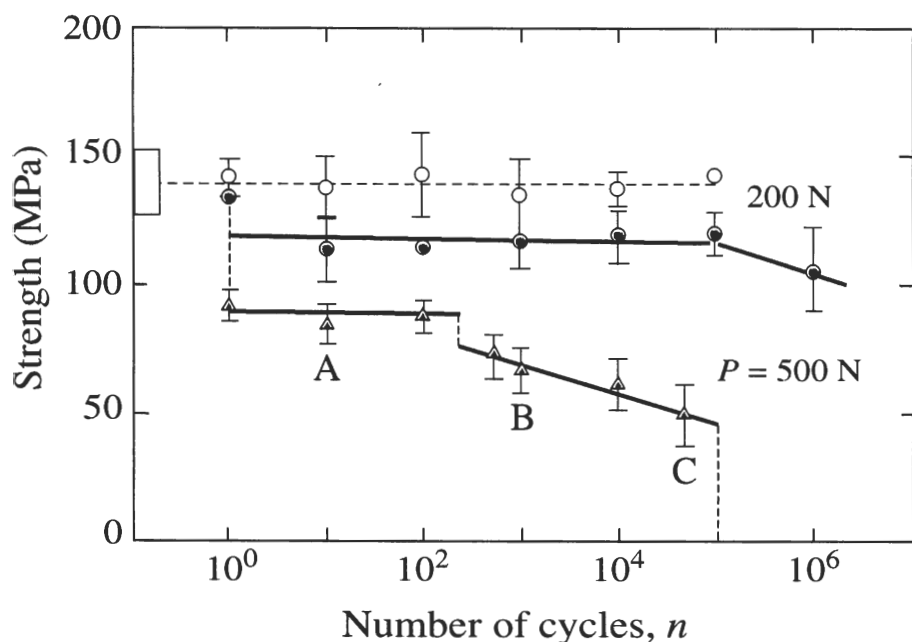
Figure 1. Inert strength as a function of number of contact cycles *n* for porcelain. Indentation with WC spheres (*r* = 3.18 mm) at maximum loads *P* indicated, in water. Data points are means and standard deviations, minimum 5 specimens *per* point. Unfilled symbols indicate failures from natural flaws, filled symbols failures from indentation sites. Box at left axis indicates "laboratory" strengths (unindented specimens). Reflected light micrographs (Nomarski illumination) in lower panel show surface failure sites at points A, B, and C marked on plot in upper panel (flexural tension axis horizontal).

are seen to suffer substantial losses—in some instances quite abruptly—at critical values of *n*. Included as the lower panels in Figs. 1 and 3-5 are surface reflection micrographs showing indentation failure sites.

Feldspathic Porcelain (Fig. 1)

Data for porcelain are shown at two contact loads, *P* = 200 N and 500 N. At *P* = 500 N, the strength shows two abrupt drops. The first such drop occurs at *n* = 1, corresponding to generation of a substantial cone crack in the first cycle. Any subsequent degradation up to *n* ≈ 10^2 cycles is imperceptible. Beyond *n* ≈ 10^2-10^3, the strength appears to undergo a second, smaller abrupt drop. The degradation thereafter is clearly accelerated, with strength at *n* = 5 x 10^4 down to ≈ 35% its original value. This degradation behavior may be correlated with the flexural fracture paths in micrographs A, B, and C. In A, just prior to the second decrement, the contact damage indicates classic cone cracks—the resulting fracture path is located clearly outside the contact, consistent with failure initiation from the subsurface cone base. In B, just beyond the second decrement, the damage

has become much more severe, and the trace of the fracture path in the flexure surface has correspondingly moved well inside the contact circle. Several near-concentric ring cracks are now evident in an annular damage region within the contact circle, with some surface chipping. In micrograph C, the contact damage area is severely enlarged, indicating gross material removal from the upper surface—in this instance, pulverized debris was observed inside and around the contact before the surface was cleaned for microscopy. Faint traces of radial cracks extending from the damage zone are also observed in micrograph C. At yet higher numbers of cycles, *n* ≈ 10^5, the specimens actually failed during the contact itself, effectively reducing the strength to zero.

At the lower contact load, *P* = 200 N, the strengths are bimodal over the bulk of the cyclic range, either remaining at the level for unindented specimens, corresponding to failures from natural flaws, or dropping by 20 to 30%, corresponding to failures from indentation sites. These results indicate that the contact load is just at the threshold of ring cracking, and that the distributions in the flaw populations which lead to that cracking are broad. The rate of strength fall-off for those specimens that do fail from indentations is imperceptibly small at first, but shows signs of acceleration at *n* ≈ 10^6. In this latter high *n* region, examination of the upper fracture surfaces again indicated a small change in fracture path from just outside to just inside the contact.

Fig. 2 compares strength data for surfaces subjected to cyclic contact tests at *n* = 10^1, 10^3, and 10^5 cycles with analogous static contact tests at equivalent hold times (*i.e.*, for *t* = *nf*), at chosen maximum load *P* = 500 N. Whereas the strengths for cyclic contacts fall off precipitously with increasing test time (ultimately to zero at *n* ≈ 10^5 cycles), the strengths for static contacts remain comparatively insensitive to time. The surfaces in the static tests showed no signs of any inner-contact damage of the kind observed in the micrographs B and C in Fig. 3.

Micaceous Glass-Ceramic (Fig. 3)

In MGC, the strength degradation shows analogous broad trends at the same loads, *P* = 200 N and 500 N, but with a higher degradation rate. For indentations at *P* = 500 N, the strength again falls off immediately and abruptly at *n* ≈ 1 cycle, and imperceptibly thereafter up to the second decrement at *n* ≈ 2.5 x 10^4 cycles. Beyond this second decrement, the strength degrades rapidly, ultimately down to ≈ 25% its original value, *i.e.*, considerably more pronounced than for the porcelain in Fig. 1. Micrographs A and B again reveal this second transition to be

Figure 2. Comparison of inert strengths of porcelain after contact with WC spheres ($r = 3.18$ mm), at maximum load $P = 500$ N: black bars, cyclic contact for n cycles at frequency f; grey bars, static contact for equivalent testing times $t = nf$ at maximum load; unfilled bar, single-cycle loading ($n = 1$ cycle); unfilled box at left axis, "laboratory" strength ($n = 0$ cycles; unindented specimens). Cyclic data reproduced from Fig. 1. Error bars indicate standard deviation, minimum 5 specimens *per* bar.

marked by the onset of enhanced annular damage within the contact area, with corresponding shift in fracture path from coincidence with the outer edge to the interior of the contact. Relative to the porcelain in Fig. 1, however, note the absence of apparent pre-existing ring cracking in micrograph A, and, conversely, enhanced radial cracking in micrograph B. At very high numbers of cycles, $n \approx 5 \times 10^5$ cycles (micrograph C), severe damage with material removal is again observed.

At $P = 200$ N, the strength shows no loss up to $n \approx 10^4$ cycles, with failures occurring from natural flaws; beyond this point, the loss is again more abrupt than in the porcelain, and failure initiates at the contact edges, much as in micrograph A. At $n \approx 5 \times 10^5$ cycles, the strength undergoes its second abrupt loss, and the failure path once more traverses the contact area.

Glass-infiltrated Alumina (Fig. 4)

The glass-infiltrated alumina has initial strength higher than that of either the porcelain or the MGC, and requires much higher loads and larger numbers of cycles to cause strength degradation. At $P = 1000$ N, a drop in strength occurs during the first cycle, with corresponding failure again from the contact edge (micrograph A; *cf*. Fig. 3A for MGC). A second drop then occurs at $n \approx 10^5$ cycles, with transition of the fracture path from the edge to the interior of the contact (micrograph B). Beyond this point, the strength loss accelerates until, at $n > 10^5$ cycles, surface spalling once more becomes apparent (micrograph C). Ultimately, at $n \approx 10^6$ cycles, failure occurs during the cyclic contact process itself.

At load $P = 500$ N, failure occurs from natural flaws up to $n \approx 10^5$ cycles, beyond which the strength drops again, with failure at or within the contact impression edge. Similarly, at $P = 200$ N, a strength drop occurs at $n \approx 10^6$ cycles. At neither of these two loads is a second strength decrement observed over the range of n covered.

Yttria-stabilized Tetragonal Zirconia Polycrystal (Fig. 5)

Y-TZP is the strongest material investigated in this study. At very high contact load, $P = 3000$ N, the strength drops abruptly beyond $n \approx 10^4$ cycles, to less than half its original value, with failure during actual contact at $n \approx 5 \times 10^5$ cycles.
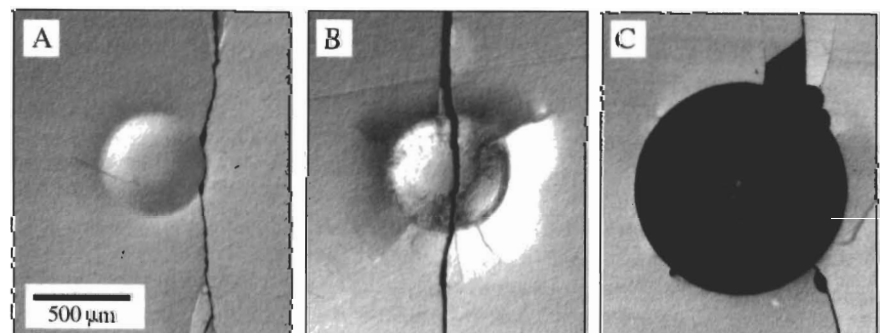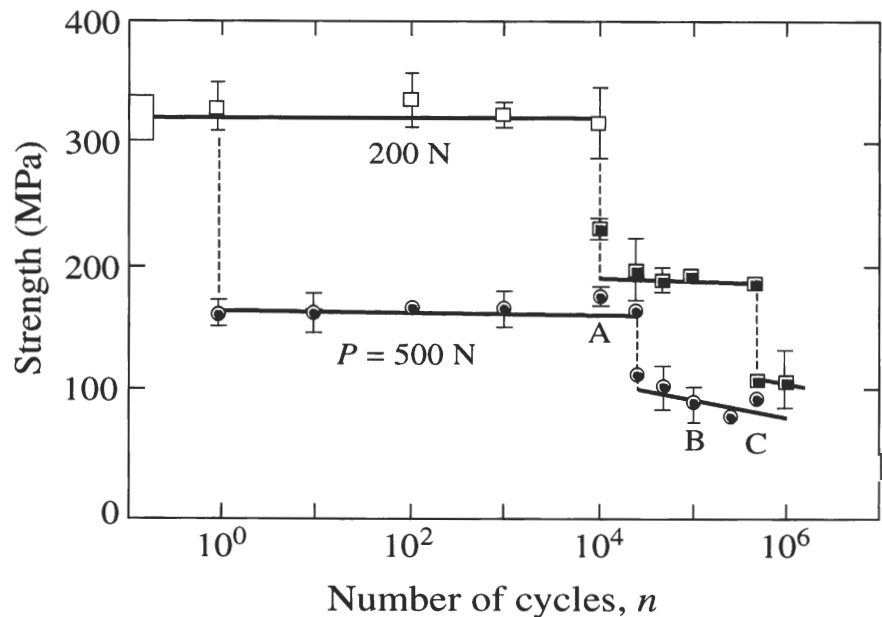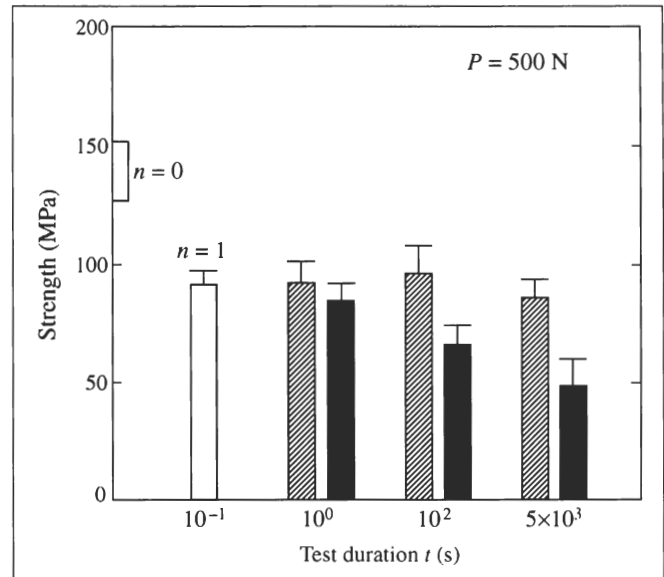

Figure 3. Inert strength as a function of number of contact cycles n for MGC. Indentation with WC spheres ($r = 3.18$ mm) at maximum loads P indicated, in water. Data points are means and standard deviations, minimum 5 specimens *per* point. Unfilled symbols indicate failures from natural flaws, filled symbols failures from indentation sites. Box at left axis indicates "laboratory" strengths (unindented specimens). Reflected light micrographs (Nomarski illumination) in lower panel show surface failure sites at points A, B, and C marked on plot in upper panel (flexural tension axis horizontal).
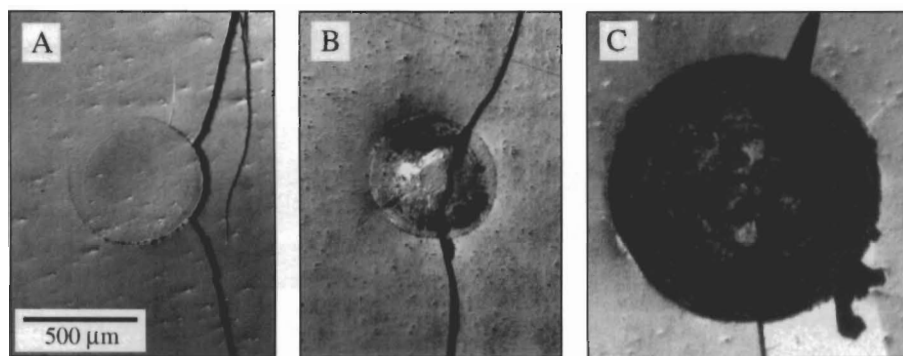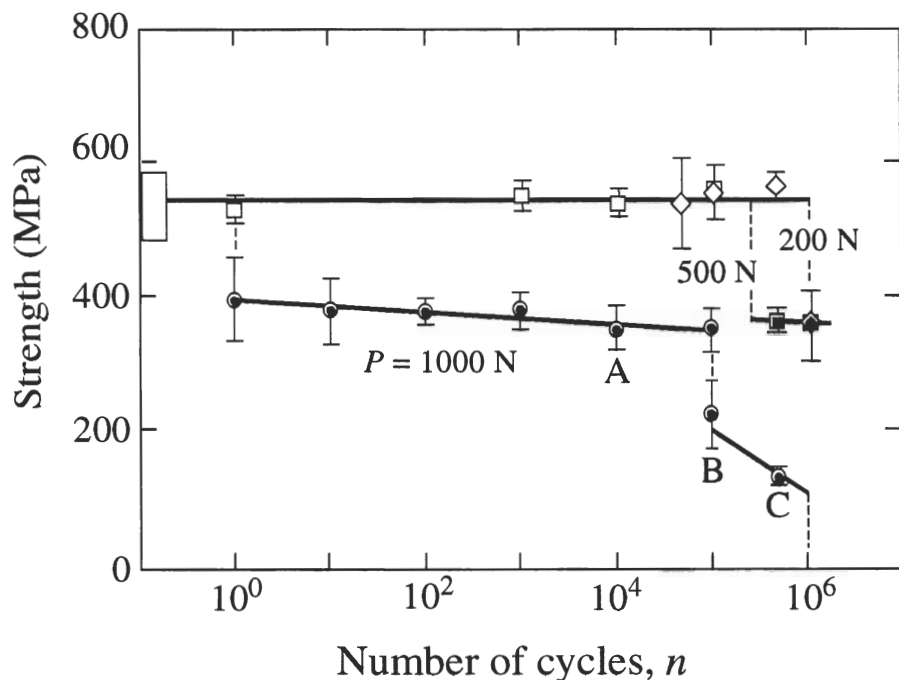
Figure 4. Inert strength as a function of number of contact cycles n for glass-infiltrated alumina. Indentation with WC spheres (r = 3.18 mm) at maximum loads P indicated, in water. Data points are means and standard deviations, minimum 5 specimens per point. Unfilled symbols indicate failures from natural flaws, filled symbols failures from indentation sites. Box at left axis indicates "laboratory" strengths (unindented specimens). Reflected light micrographs (Nomarski illumination) in lower panel show surface failure sites at points A, B, and C marked on plot in upper panel (flexural tension axis horizontal).

1) and multi-cycle-indented ($n = 10^6$) over the cycle range covered. (Values of p for Y-TZP are not available, because no failures occurred from damage sites over the range of test conditions covered in these analyses.)

Table 2 shows ANOVA results of analyses on data from Fig. 2 for porcelain at contact load $P = 500$ N, comparing strengths in single-cycle loading ($t = 0.1$ sec) with those at extended contact durations t in both cyclic and static loading. Whereas the strengths show no significant loss with increasing time ($t = 1$ to 5×10^3 sec) in the static contact loading, degradation becomes highly significant in the cyclic loading at $t \gg 10^2$ sec. Table 2 also shows ANOVA results on the same data, this time directly comparing static and cyclic data at each specified value of t. This analysis confirms the susceptibility of the strength data to cyclic fatigue.

The transition in damage mode responsible for the ultimate strength degradation in Figs. 1 and 3-5, with its attendant shift in flexure failure path from outer tangential to inner radial origin relative to the contact circle, points to an increasing role of radial cracking in the lifetime characteristics. Fig. 6 shows transmission micrographs of radial cracks in back-thinned porcelain, MGC, and alumina specimens (recall that the Y-TZP is too opaque for similar observation), in each case for contact conditions beyond the onset of the second strength decrement. In the MGC, these cracks appear to be associated with dark zones of subsurface damage beneath and around the outer contact region. Note also the persistent appearance of circumferential surface ring crack traces at the contact periphery, although these traces are relatively faint and somewhat segmented in the relatively quasi-plastic MGC material (Fig. 6B).

DISCUSSION

In this paper, we have demonstrated the effect of multi-cycle sphere-contact loading on the surface condition and long-term strength of a broad range of dental ceramics—porcelain, micaceous glass-ceramic (MGC), glass-infiltrated alumina, and yttria-stabilized tetragonal zirconia polycrystal (Y-TZP)—in water. Damage accumulates from repeated contacts, even at loads considerably lower than those needed to produce single-cycle degradation, and ultimately limits the useful life of the structure. The deterioration in strength can be abrupt at critical numbers of cycles as different mechanisms of damage accumulation come progressively into play. Such deterioration occurs in all materials tested, most rapidly and at lower contact loads in the aesthetic ceramics (porcelain and MGC) but even to

The annular damage within the contact shows a trend similar to that in the alumina, with transition in failure path from the contact edge (micrograph A) to the contact interior (micrograph B), with attendant damage build-up in the latter case. However, in this material, a second drop in strength is not achieved at any load over the range of n covered. No strength loss at all is observed at $P \approx 500$ N over the data range.

One-way ANOVA is used to quantify the significance of strength differentials in Figs. 1-5. Such differentials are considered significant if $p < 0.05$, insignificant if $p > 0.05$. Table 1 shows the results of analyses on selected cyclic fatigue data for each material, at contact loads $P = 200$ N for the aesthetic ceramics and $P = 500$ N for the structural (core) ceramics. The listed p values confirm insignificant initial strength losses between unindented ($n = 0$) and single-cycle-indented ($n = 1$) specimens at the loads chosen, but highly significant subsequent losses between single-cycle-indented ($n =$

some degree in the stronger and tougher structural ceramics (glass-infiltrated alumina and Y-TZP). Material inter-comparisons are more readily made on the "master map" of Fig. 7, condensed from selected strength data from Figs. 1 and 3-5: for the aesthetic ceramics, data at P = 200 N; for the structural core ceramics, data at P = 500 N. It is clear that while the structural materials are likely to survive even the most demanding contact histories, the two aesthetic ceramics fall within the danger region of attainable biting forces ($P \approx 200$ N). Note that the MGC, although initially twice as strong as the porcelain, ultimately drops to nearly the same strength at large n—the MGC is demonstrably more susceptible to degradation, a fact attributable to its much greater susceptibility to *quasi*-plastic deformation (Peterson *et al.*, 1998a,b).

Comparative fatigue tests on the porcelain (Fig. 2) confirm that cyclic loading is much more deleterious than static loading under conditions of equivalent hold time at the same maximum load. If damage accumulation were to be attributed solely to chemically enhanced slow crack growth, as is often presumed for ideally brittle materials in purely tensile applied stresses (Evans and Fuller, 1974), the accumulation would actually be greater in the static fatigue (or even dynamic fatigue) loading than in the cyclic fatigue, because of a higher time-average in active stress intensity. The converse result observed here and elsewhere (White *et al.*, 1995, 1997; Lee and Lawn, 1999) indicates a dominant mechanical component in the build-up of the contact damage.

Accordingly, long lifetimes in tougher dental ceramics are ultimately limited by the evolution of the *quasi*-plastic damage mode. Initially, for small numbers of cycles n at low loads P, loss in strength may occur at some critical n, in some cases quite precipitously. This level of damage may not in itself lead to immediate failure—moreover, subsequent decline in strength with further increase in n tends to be modest, until the onset of the more severe damage modes. In the initial regions, the damage modes are quite distinctive in the different materials (Peterson *et al.*, 1998a). The more brittle porcelain shows well-defined ring and cone cracks outside the contact. The more *quasi*-plastic materials, especially MGC but also Y-TZP (and, to a lesser extent, alumina), show well-defined surface impressions, akin to conventional hardness impressions in ideally plastic materials. Surface ring cracks may also form in these latter materials, but various micromechanisms inhibit penetration into deep cone cracks: constrained deflection along the weak grain boundaries in the MGC (Lee *et al.*, 1997) (recall the faint, segmented ring cracks in Fig. 6B); and stress relief from microplasticity, including a tetragonal-to-monoclinic phase transformation in zirconia (Green *et al.*, 1989; Pajares *et*
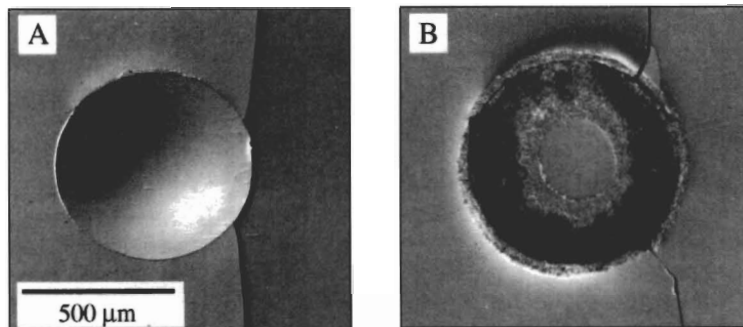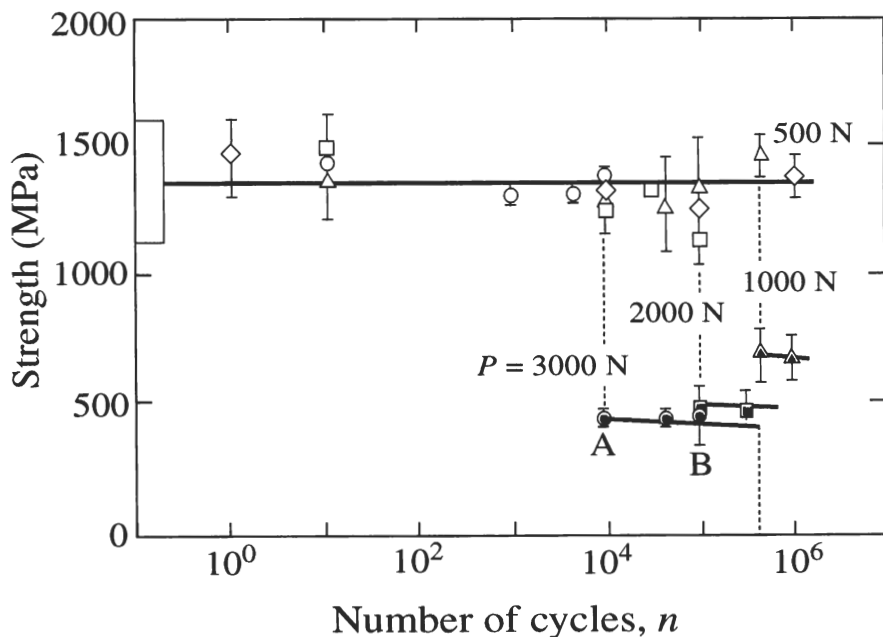

Figure 5. Inert strength as a function of number of contact cycles n for Y-TZP. Indentation with WC spheres (r = 3.18 mm) at maximum loads P indicated, in water. Data points are means and standard deviations, minimum 5 specimens *per* point. Unfilled symbols indicate failures from natural flaws, filled symbols failures from indentation sites. Box at left axis indicates "laboratory" strengths (unindented specimens). Reflected light micrographs (Nomarski illumination) in lower panel show surface failure sites at points A and B marked on plot in upper panel (flexural tension axis horizontal).

al., 1995a). The difference in damage modes is also reflected in the flexural failure paths in the pertinent micrographs, those labeled A in Figs. 1 and 3-5. In the porcelain (Fig. 3A), failure originates outside the surface ring crack, consistent with brittle failure from the cone crack base (Lawn *et al.*, 1998; Lee and Lawn, 1998). In the other ceramics (Figs. 3A, 4A, 5A), failure originates from the circumference of the seemingly homogeneous plastic surface impressions—no ring cracks were observed prior to flexure in these latter cases, suggesting failure from a weakened interface at the boundary between the severely deformed plastic zone and its elastic surrounds.

At greater n and higher P, damage develops progressively in an annulus within the contact circle. In the porcelain, this damage takes the appearance of an ever-increasing density of concentric inner ring cracks, with pulverized, powdery debris inside the (as-indented, uncleaned) contact area. In the other, more *quasi*-plastic ceramics, the damage is more reminiscent of "fretting" (Johnson, 1985; Kennedy *et al.*, 1994), with attendant surface flaking and, subsequently, mass removal. The debris

Table 1. One-way ANOVA Analysis of Cyclic Fatigue Data in Figs. 1, 3, 4, and 5 for Dental Ceramics, at Loads *P* Specified

Materials	n_1 Cycles[a]	n_2 Cycles[a]	*p*
Porcelain (*P* = 200 N)	0[b]	1	0.9
	1	10^6	0.0001
MGC (*P* = 200 N)	0	1	0.1
	1	10^6	1×10^{-6}
Alumina (*P* = 500 N)	0	1	0.7
	1	10^6	7×10^{-5}
Y-TZP (*P* = 500 N)	0	1	NA
	1	10^6	

[a] Comparing significance of strength differences: between $n_1 = 0$ (unindented) and $n_2 = 1$ (single-cycle); between $n_1 = 1$ (single-cycle) and $n_2 = 10^6$ (maximum cycles tested).
[b] Tested as-polished (unindented).

Table 2. One-way ANOVA Analysis of Data for Indented Porcelain Specimens[a], Comparing Data Under Different Testing Conditions

t	10^0 Sec	10^2 Sec	5×10^3 Sec
p ($n = 1$,S)[b]	0.9	0.3	0.2
p ($n = 1$,C)[c]	0.03	0.05	0.006
p (S,C)[d]	0.05	0.001	0.0004

[a] Indentation load *P* = 500 N (*cf.* Figs. 1 and 2). Comparison of strength differences between testing states:
[b] Single-cycle test *n* = 1 (contact duration 0.1 sec), and static fatigue test S at specified contact durations *t*.
[c] Single-cycle test *n* = 1 (contact duration 0.1 sec), and cyclic fatigue test C at specified contact durations *t*.
[d] Static fatigue test S and cyclic fatigue test C, at specified contact durations *t*.

remains trapped at the indentation site during the contact, and could lead to accelerated damage accumulation and wear. Cracking in the region under the indenter would lower the local modulus, leading to increased penetration of the indentor and expansion of the contact area. Despite any associated reduction in contact pressure, the damage accumulation continues to accelerate. The annular damage region in all cases is bounded by the outer and inner contact radii at the maximum and minimum cyclic loads. Using the classic Hertzian relation between contact radius *a* and load *P*, $a \propto P^{1/3}$ (Hertz, 1896; Johnson, 1985), and inserting $P_{min}/P_{max} \approx 0.040$ (20 N/500 N), we obtain $a_{inner}/a_{outer} = 0.33$, consistent with the relative scale of the annular zone in the micrographs for porcelain and MGC in Figs. 1 and 3. It is pertinent to recall that no such inner annular damage is observed in the static fatigue tests. It would appear that the damage is associated in some manner with a periodically expanding and contracting contact circle, augmented by the access of environmental water into the re-contact zone.

Regardless of material type, the inner damage eventually builds up to a sufficient intensity to initiate outwardly spreading radial cracks (Fig. 6), the more rapidly the higher load, with ensuing rapid demise in surface integrity. These radial cracks

are responsible for the second decrement in strength observed in Figs. 1 and 3-5. Radial cracks are more typically associated with Vickers indenters, and with *quasi*-plastic materials (Marshall and Lawn, 1979; Marshall *et al.*, 1979; Lawn, 1993). They nevertheless can be induced by spherical contacts in even the most brittle materials under sufficiently severe loading conditions, as the indenter begins to penetrate and thereby change its character from "blunt" to "sharp" (Lawn and Wilshaw, 1975; Swain and Hagan, 1976). The near-contact damage generated by the penetrating indenter provides essential nuclei for the initiation of radial and other subsurface-embryonic cracks. (An earlier study on the same alumina as in Fig. 6 showed that well-developed radial cracks from single-cycle Vickers indentations at *P* = 100 N reduced strength to $\approx$ 200 MPa [Jung *et al.*, 1999a]—by comparison, the strength values for sphere indentations at *P* = 1000 N in Fig. 4 are substantially higher at *n* = 1, but diminish below this level at *n* > 10^5, consistent with a cyclic-induced blunt-sharp transition.) Unlike ring cracks, which flare downward and outward into cones at shallow angles to the surface (Frank and Lawn, 1967; Lawn and Wilshaw, 1975; Lawn, 1993), radial cracks form perpendicular to the surface, and are thereby more deleterious (Jung *et al.*, 1999a). The same damage responsible for the crack initiation also generates, in the surrounding contact field, residual tangential tensile stresses which drive the radial cracks outward (Marshall and Lawn, 1979), thereby degrading the long-term strength still further (Marshall *et al.*, 1979).

This leaves the issue of the underlying micromechanisms of the damage accumulation modes. While these mechanisms are not yet fully understood, they are linked inextricably to the material microstructure. In the *quasi*-plastic MGC, weak interfaces between the crystalline mica platelets and bonding glass phases enable grain-boundary sliding to occur from the action of highly concentrated shear stresses
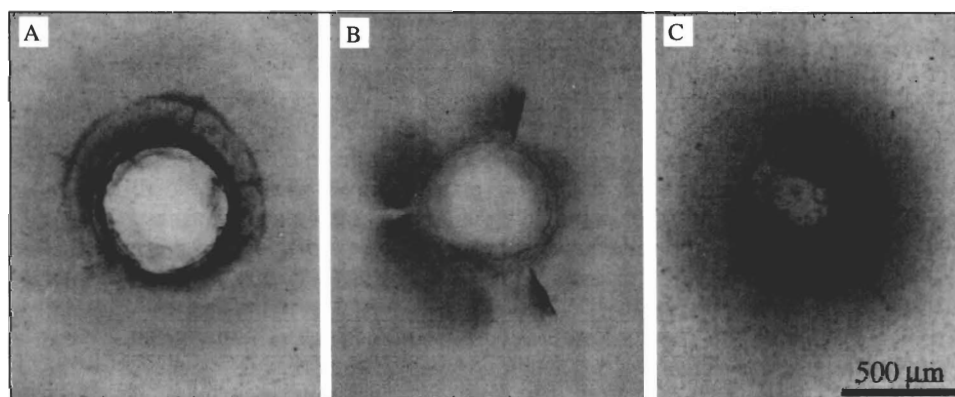

Figure 6. Views of subsurface damage in specimens thinned from back surface (*i.e.*, opposite indentation top surface), in transmitted light: (A) porcelain, *P* = 500 N, *n* = 5 x 10^3 cycles; (B) MGC, *P* = 500 N, *n* = 5 x 10^4 cycles; and (C) glass-infiltrated alumina, *P* = 1000 N, *n* = 10^5 cycles. Indentation with WC spheres (*r* = 3.18 mm). Note appearance of radially directed cracks at contact periphery.

(Chyung *et al.*, 1972; Cai *et al.*, 1994a,b; Fischer-Cripps and Lawn, 1996). This sliding can, in turn, open microcracks at the constrained platelet ends which, after repeated cycles, coalesce into macroscopic radial cracks and lead to strength degradation and easy material removal. Under cyclic loading, interfacial wear degrades the frictional crack-bridging mechanisms that make *quasi*-plastic materials relatively damage-tolerant under single-cycle loading. Localized weakness in shear is the common element in all such *quasi*-plastic ceramics, although the precise form of it can vary from material to material (Lawn *et al.*, 1994). In the more brittle materials like the glass-based porcelains, where shear deformation is much more restricted (as reflected, for instance, in relatively linear indentation stress-strain curves [Peterson *et al.*, 1998a]), the surface damage has a more crack-like appearance. Nevertheless, even glassy materials are ultimately susceptible to breakdown in shear under sufficiently severe conditions (Swain and Hagan, 1976; Hagan and Swain, 1978; Hagan, 1979, 1980), especially once the indenter begins to penetrate the material surface. Thus, although strength degradation is not as rapid in the porcelains as in the MGC, it is nonetheless manifest. Fracture mechanics models seeking to quantify the role of damage in strength determination are just beginning to be developed in the materials literature, with a focus thus far on single-cycle loading in the light damage region (Lawn *et al.*, 1998). Only a cursory understanding currently exists for the primary role of repeated loading (Guiberteau *et al.*, 1993; Cai *et al.*, 1994b; Padture and Lawn, 1995) and the subsidiary role of environmental water (Lawn *et al.*, 1983; Guiberteau *et al.*, 1993) in the micromechanical shear faulting processes responsible for the fatigue.

Consideration of the present results in the context of clinical performance of crowns and other dental restorations is an essential end goal of this work. Aesthetic ceramics (porcelain, MGC), in the form of veneers and onlays/inlays, are exposed to direct contacts with opposing teeth, and are therefore more vulnerable to damage than are structural core ceramics (alumina, zirconia). The incidence of radial cracks and other damage-induced subsurface cracks is highly degrading, and signals the end of useful material lifetime. Plastic-like impressions, while seemingly benign in their early stages, are essential precursors to this kind of deleterious cracking. But they are hard to detect unless one looks for them in sensitive (Nomarski) illumination. Again, evolution of radial cracking may begin subsurface, and may not always be easily visible without proper illumination (*e.g.*, Fig. 6). Attendant fretting damage may enhance the wear rates of both the restoration and the opposing tooth (Xu *et al.*, 1998).

Traditional methods used to predict lifetimes of ceramics, such as dynamic fatigue in which initially undamaged bend specimens are loaded continually to failure at constant crosshead speed, generate relatively low stress levels, and grow a dominant flaw to failure over an integrated time interval in an essentially tensile field. The contact test adopted here implies that failures in oral function may be more complex, especially in severe loading conditions, involving the coalescence of microcracks into a potentially damaging macroflaw within an essentially compressive field. Such coalescence processes may not be readily detectable in pre-failure (or even in post-failure) examinations of dental restorations. As shown here (*e.g.*, Fig. 2), damage accumulation processes are particularly dangerous
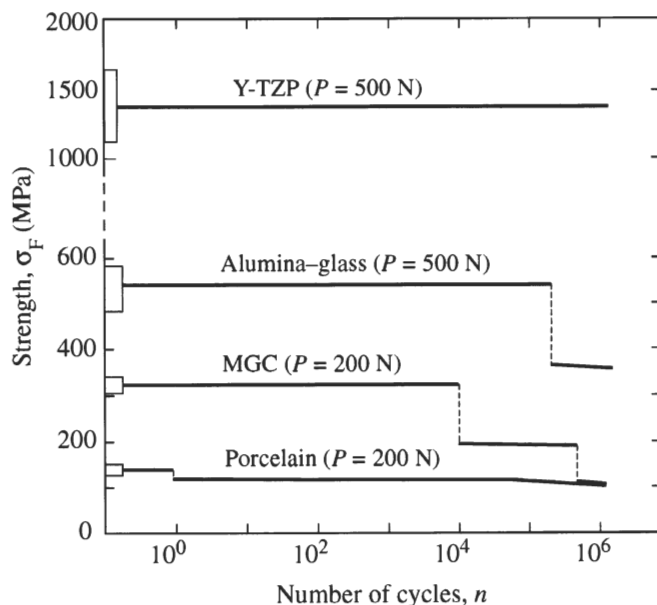

Figure 7. Master diagram comparing contact fatigue responses for the materials represented in Figs. 1, 3, 4, and 5, at load $P = 200$ N for porcelain and MGC and at $P = 500$ N for alumina and Y-TZP. (Note change of scale on upper strength axis.)

because they can greatly accelerate strength losses and reduce lifetimes relative to simple slow-crack-growth processes.

Determination of clinical failure modes in retrieved crowns is far from a precise science—data on failure modes are not exhaustive, and are subject to different interpretations (Hankinson and Cappetta, 1994; Kelly *et al.*, 1995; Kelsey *et al.*, 1995; Kelly, 1997). Worn surfaces and missing pieces may obscure clues to any early development of damage (*cf.* Figs 1C, 3C, and 4C). Identification of a "critical flaw" in a failed specimen may not in itself be sufficient to trace the evolution of damage prior to the critical event, especially if the damage lies subsurface. Although we do not assert that the damage accumulation modes described here will always constitute the source of clinical failure, such modes are particularly dangerous, and the designer should be aware of them in any materials selection and development process.

Accordingly, contact fatigue testing with spherical indenters offers a means of characterizing and quantifying prospective materials for restorative applications. Such testing compellingly demonstrates the need to evaluate strength properties *after* as well as *before* a repeat-loading regimen. The test itself is uniquely simple to perform, and captures the essence of tooth contact. It may be argued that real dental function involves lateral as well as normal biting forces (DeLong and Douglas, 1983), and that these lateral forces may greatly exacerbate the evolution of damage. This is demonstrably true (Lawn, 1967)—but simple normal loading enables one to separate material properties from dental mechanics with the minimum of complication, in a configuration accessible to any routine testing laboratory. It may also be argued that real dental restorations involve layer rather than monolithic material structures (Jung *et al.*, 1999b; Tsai *et al.*, 1998). This is also undeniable, but a fundamental description of any composite structure cannot proceed unless the properties of the component parts are first understood.

Extension of contact testing to evaluation of the fatigue properties of dental layer structures, including, ultimately, actual crown configurations themselves, is envisaged as a logical extension of the contact testing protocol.

ACKNOWLEDGMENTS

REFERENCES

Anusavice KJ (1989). Criteria for selection of restorative materials: properties vs technique sensitivity. In: Quality evaluations of dental restorations. Anusavice KJ, editor. Chicago: Quintessence, pp. 15-56.

Cai H, Stevens Kalceff MA, Lawn BR (1994a). Deformation and fracture of mica-containing glass-ceramics in Hertzian contacts. *J Mater Res* 9:762-770.

Cai H, Kalceff MAS, Hooks BM, Lawn BR, Chyung K (1994b). Cyclic fatigue of a mica-containing glass-ceramic at Hertzian contacts. *J Mater Res* 9:2654-2661.

Chyung CK, Beall GH, Grossman DG (1972). Microstructures and mechanical properties of mica glass-ceramics. In: Electron microscopy and structure of materials. Thomas G, Fulrath RM, Fisher RM, editors. Berkeley, CA: University of California Press, pp. 1167-1194.

Craig RG (1997). Mechanical properties. In: Restorative dental materials. Chapter 4. Craig RG, editor. St. Louis: Mosby.

Dauskardt RH, Marshall DB, Ritchie RO (1990). Cyclic fatigue-crack propagation in magnesia-partially-stabilized zirconia ceramics. *J Am Ceram Soc* 73:893-903.

DeLong R, Douglas WH (1983). Development of an artificial oral environment for the testing of dental restoratives: bi-axial force and movement control. *J Dent Res* 62:32-36.

Evans AG, Fuller ER (1974). Crack propagation in ceramic materials under cyclic loading conditions. *Metall Trans* 5:27-33.

Fairhurst CW, Lockwood PE, Ringle RD, Twiggs SW (1993). Dynamic fatigue of feldspathic porcelain. *Dent Mater* 9:269-273.

Fischer-Cripps AC, Lawn BR (1996). Stress analysis of contact deformation in quasi-plastic ceramics. *J Am Ceram Soc* 79:2609-2618.

Frank FC, Lawn BR (1967). On the theory of Hertzian fracture. *Proc R Soc Lond* 299(A):291-306.

Giordano RA (1996). Dental ceramic restorative systems. *Compend Contin Educ Dent* 17:779-782, 784-786.

Green DJ, Hannink RHJ, Swain MV (1989). Transformation toughening of ceramics. Boca Raton, FL: CRC Press.

Guiberteau F, Padture NP, Cai H, Lawn BR (1993). Indentation fatigue: a simple cyclic Hertzian test for measuring damage accumulation in polycrystalline ceramics. *Philos Mag* 68(A):1003-1016.

Hagan JT (1979). Micromechanics of crack nucleation during

indentations. *J Mater Sci* 14:2975-2980.

Hagan JT (1980). Shear deformation under pyramidal indenters in soda-lime glass. *J Mater Sci* 15:1417-1424.

Hagan JT, Swain MV (1978). The origin of median and lateral cracks at plastic indents in brittle materials. *J Physics: D* 11:2091-2102.

Hankinson JA, Cappetta EG (1994). Five-years' clinical experience with a leucite-reinforced porcelain crown system. *Int J Periodont Rest Dent* 14:138-153.

Hertz H (1896). Hertz's miscellaneous papers. Chapters 5, 6. London: Macmillan.

Johnson KL (1985). Contact mechanics. London: Cambridge University Press.

Jung YG, Peterson IM, Pajares A, Lawn BR (1999a). Contact damage resistance and strength degradation of glass-infiltrated alumina and spinel ceramics. *J Dent Res* 78:804-814.

Jung YG, Wuttiphan S, Peterson IM, Lawn BR (1999b). Damage modes in dental layer structures. *J Dent Res* 78:887-897.

Kelly JR (1997). Ceramics in restorative and prosthetic dentistry. *Ann Rev Mater Sci* 27:443-468.

Kelly JR, Tesk JA, Sorensen JA (1995). Failure of all-ceramic fixed partial dentures *in vitro* and *in vivo*: analysis and modeling. *J Dent Res* 74:1253-1258.

Kelsey WP 3rd, Cavel T, Blankenau RJ, Barkmeier WW, Wilwerding TM, Latta MA (1995). 4-year clinical study of castable ceramic crowns. *Am J Dent* 8:259-262.

Kennedy PJ, Conte AA, Whitenton EP, Ives LK, Peterson MB (1994). Surface damage and mechanics of fretting wear in ceramics. In: Friction and wear of ceramics. Jahanmir S, editor. New York: Marcel Dekker, pp. 79-98.

Lathabai S, Lawn BR (1989). Fatigue limits in noncyclic loading of ceramics with crack-resistance curves. *J Mater Sci* 24:4298-4306.

Lathabai S, Mai Y-W, Lawn BR (1989). Cyclic fatigue behavior of an alumina ceramic with crack-resistance curves. *J Am Ceram Soc* 72:1760-1763.

Lathabai S, Rödel J, Lawn BR (1991). Cyclic fatigue from frictional degradation at bridging grains in alumina. *J Am Ceram Soc* 74:1340-1348.

Lawn BR (1967). Partial cone crack formation in a brittle material loaded with a sliding indenter. *Proc R Soc Lond* 299(A):307-316.

Lawn BR (1993). Fracture of brittle solids. Cambridge: Cambridge University Press.

Lawn BR, Wilshaw TR (1975). Indentation fracture: principles and applications. *J Mater Sci* 10:1049-1081.

Lawn BR, Dabbs TP, Fairbanks CJ (1983). Kinetics of shear-activated indentation crack initiation in soda-lime glass. *J Mater Sci* 18:2785-2797.

Lawn BR, Padture NP, Cai H, Guiberteau F (1994). Making ceramics 'ductile'. *Science* 263:1114-1116.

Lawn BR, Lee SK, Peterson IM, Wuttiphan S (1998). A model of strength degradation from Hertzian contact damage in tough ceramics. *J Am Ceram Soc* 81:1509-1520.

Lee SK, Lawn BR (1998). Role of microstructure in Hertzian contact damage in silicon nitride: II. Strength degradation. *J Am Ceram Soc* 81:997-1003.

Lee SK, Lawn BR (1999). Contact fatigue in silicon nitride. *J Am Ceram Soc* 82:1281-1288.

Lee SK, Wuttiphan S, Lawn BR (1997). Role of microstructure in Hertzian contact damage in silicon nitride: I. Mechanical characterization. *J Am Ceram Soc* 80:2367-2381.

Marshall DB, Lawn BR (1979). Residual stress effects in sharp-contact cracking: I. Indentation fracture mechanics. *J Mater Sci* 14:2001-

2012.

Marshall DB, Lawn BR (1980). Flaw characteristics in dynamic fatigue: the influence of residual contact stresses. *J Am Ceram Soc* 63:532-536.

Marshall DB, Lawn BR, Chantikul P (1979). Residual stress effects in sharp-contact cracking: II. Strength degradation. *J Mater Sci* 14:2225-2235.

Padture NP, Lawn BR (1995). Fatigue in ceramics with interconnecting weak interfaces: a study using cyclic Hertzian contacts. *Acta Metall* 43:1609-1617.

Pajares A, Guiberteau F, Lawn BR, Lathabai S (1995a). Hertzian contact damage in magnesia-partially-stabilized zirconia. *J Am Ceram Soc* 78:1083-1086.

Pajares A, Wei L, Lawn BR, Marshall DB (1995b). Damage accumulation and cyclic fatigue in Mg-PSZ at Hertzian contacts. *J Mater Res* 10:2613-2625.

Peterson IM, Pajares A, Lawn BR, Thompson VP, Rekow ED (1998a). Mechanical characterization of dental ceramics by Hertzian contacts. *J Dent Res* 77:589-602.

Peterson IM, Wuttiphan S, Lawn BR, Chyung K (1998b). Role of microstructure on contact damage and strength degradation of micaceous glass-ceramics. *Dent Mater* 14:80-89.

Phillips RW (1991). Skinner's science of dental materials. Philadelphia: W.B. Saunders.

Ritchie RO (1988). Mechanisms of fatigue crack propagation in metals, ceramics, composites: role of crack-tip shielding. *Mater Sci Eng* 103(A):15-28.

Ritter JE (1978). Engineering design and fatigue failure of brittle materials. In: Fracture mechanics of ceramics. Bradt RC, Lange FF, Hasselman DPH, editors. New York: Plenum, pp. 667-686.

Suresh S (1991). Fatigue of materials. Cambridge: Cambridge University Press.

Swain MV, Hagan JT (1976). Indentation plasticity and the ensuing fracture of glass. *J Phys D: Appl Phys* 9:2201-2214.

Tsai YL, Petsche PE, Anusavice KJ, Yang MC (1998). Influence of glass-ceramic thickness on Hertzian and bulk fracture mechanisms. *Int J Prosthodont* 11:27-32.

Wheeler RC (1958). A textbook of dental anatomy and physiology. Philadelphia, PA: W.B. Saunders.

White SN, Zhao XY, Zhaokun Y, Li ZC (1995). Cyclic mechanical fatigue of a feldspathic dental porcelain. *Int J Prosthodont* 8:413-420.

White SN, Li ZC, Yu Z, Kipnis V (1997). Relationship between static chemical and cyclic mechanical fatigue in a feldspathic porcelain. *Dent Mater* 13:103-110.

Wiederhorn SM (1967). Influence of water vapor on crack propagation in soda-lime glass. *J Am Ceram Soc* 50:407-414.

Xu HH, Smith DT, Jahanmir S, Romberg E, Kelly JR, Thompson VP, *et al.* (1998). Indentation damage and mechanical properties of human enamel and dentin. *J Dent Res* 77:472-480.